LANGMUIR

Article

pubs.acs.org/Langmuir

# Organic Monolayers by $B(C_6F_5)_3$-Catalyzed Siloxanation of Oxidized Silicon Surfaces

Jorge Escorihuela,[†] Sidharam P. Pujari,[†] and Han Zuilhof*[,†,‡]

[†]Laboratory of Organic Chemistry, Wageningen University and Research, Stippeneng 4, 6708 WE Wageningen, The Netherlands

[‡]Department of Chemical and Materials Engineering, King Abdulaziz University, Jeddah, Saudi Arabia

Supporting Information

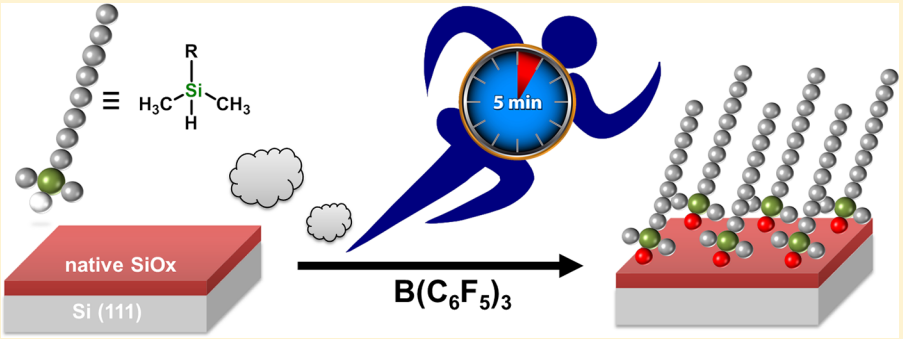


**ABSTRACT:** Inspired by the homogeneous catalyst tris(pentafluorophenyl) borane [$B(C_6F_5)_3$], which acts as a promotor of Si−H bond activation, we developed and studied a method of modifying silicon oxide surfaces using hydrosilanes with $B(C_6F_5)_3$ as the catalyst. This dehydrosiloxanation reaction yields complete surface coverage within 10 min at room temperature. Organic monolayers derived from hydrosilanes with varying carbon chain lengths ($C_8$−$C_{18}$) were prepared on oxidized Si(111) surfaces, and the thermal and hydrolytic stabilities of the obtained monolayers were investigated in acidic (pH 3) medium, basic (pH 11) medium, phosphate-buffered saline (PBS), and deionized water (neutral conditions) for up to 30 days. DFT calculations were carried out to gain insight into the mechanism, and the computational results support a mechanism involving silane activation with $B(C_6F_5)_3$. This catalyzed reaction path proceeds through a low-barrier-height transition state compared to the noncatalyzed reaction path.

## INTRODUCTION

Surface functionalization of inorganic substrates such as silicon oxides ($SiO_x$) and glass has been the focus of much attention and effort in the past few decades because of the potential applications of the functionalized materials in biomedicine,[1,2] diagnostics and biosensing,[3,4] surface chemistry,[5] photonics,[6] photovoltaics,[7] and electronics.[8] Among the different strategies for functionalizing silicon substrates, two approaches are frequently used. One is based on the attachment of organic self-assembled monolayers (SAMs),[9,10] and the other is based on the deposition of multilayers or polymeric compounds.[11,12] Although both approaches have significant potential, the attachment of SAMs is commonly preferred as it allows for the easy and highly controllable tuning of the surface properties and functionality.[13]

The most common approaches used to prepare organic monolayers on silicon oxide surfaces[14] involve the reaction between silanol groups (Si−OH) present on the oxidized silicon surface and functionalized organosilicon compounds, such as chlorosilanes,[15] dimethylaminosilanes,[16] alkoxysilanes,[17,18] and allylsilanes[19,20] to form stable siloxane (Si−O−Si) bonds, although other methods for obtaining covalently bound organic monolayers are also increasingly being explored.[21−23] Despite the simplicity of these approaches, uniform monolayers are difficult to obtain using solution-phase deposition methods, and undesirable polysiloxane networks are often formed.[24,25] In addition, these surface modification approaches often require long reaction times, commonly taking 2−24 h.[26] Silicon nanowires (SiNWs) can function as a specific example. SiNWs are quasi-one-dimensional structures with diameters of less than 100 nm, resulting in high surface-to-volume ratios.[27] Because of these high ratios and their unique quasi-one-dimensional electronic structures, SiNW-based devices have properties that can outperform those of their traditional counterparts in many potential applications in the design of sensors,[28] solar cells,[29,30] Li-ion batteries,[31] and superhydrophobic surfaces.[32] Most modification processes for oxidized SiNW are based on silanization,[33] esterification,[34] and phosphonate attachment reactions,[35] although hydrosilylation in particular has been used heavily for oxide-free H-terminated SiNWs.[36−38] Each of these functionalization approaches typically requires at least several hours (sometimes even

**Received:** January 12, 2017
**Revised:** February 13, 2017
**Published:** February 23, 2017

  

DOI: 10.1021/acs.langmuir.7b00110
*Langmuir* 2017, 33, 2185−2193

**Scheme 1. Schematic Representation of $B(C_6F_5)_3$-Catalyzed Grafting of Hydrosilane Derivatives (1−5) onto Oxidized Si(111) Surfaces**

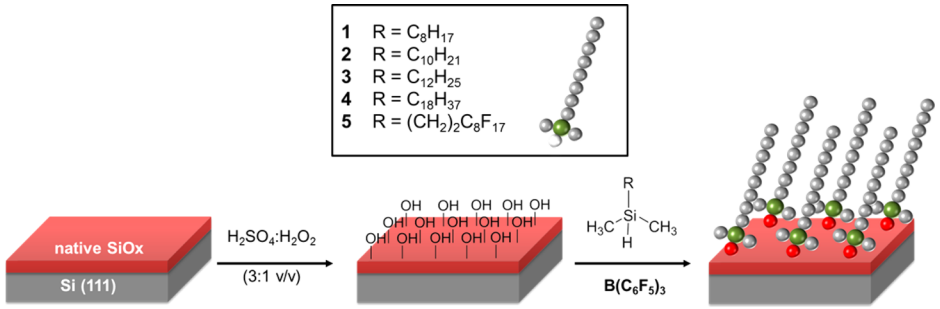


overnight) and often also elevated temperatures to reach completion, which strongly limits scale-up and concomitant industrial applications. Therefore, the quest for novel rapid and high-quality surface modification strategies is of utmost interest.

Recently, surface modification of silica[39] and porous silicon[40] based on the grafting of hydrosilanes using tris(pentafluorophenyl)borane [$B(C_6F_5)_3$] as a catalyst—formally a dedihydrosiloxanation—has gained interest, specifically becuause of its short reaction times (minutes rather than hours). Given the evident relevance of this reaction, we were thus interested in both the mechanism of formation and the stability of any formed monolayers. In fact, the stability of this organic monolayer, which is a crucial parameter in the performance and durability of biosensing devices,[41] has not yet been investigated at all. In the current work, we therefore focus on five goals: (1) preparation of a series of monolayers made from hydrosilanes of different alkyl lengths [$CH_3$−$(CH_2)_n$−$CH_2$−$Si(CH_3)_2$−H, $n$ = 6−16] on oxidized Si(111) using $B(C_6F_5)_3$ as the catalyst, along with detailed characterization of the resulting monolayers by X-ray photoelectron spectroscopy (XPS), infrared reflection absorption spectroscopy (IRRAS), atomic force microscopy (AFM), ellipsometry, and static contact angle (SCA) measurements; (2) study of the hydrolytic stability of the obtained monolayers under standardized conditions for stability testing [in acid (pH 3), base (pH 11), phosphate-buffered saline (PBS), and deionized water (neutral conditions), from 1 to 30 days][42] and of the thermal stability of different monolayers upon prolonged exposure to elevated temperature (130 °C); (3) study of the mechanism of the attachment reaction by quantum mechanical [M11/6-311+G(d,p)] calculations; (4) rapid preparation of patterned hydrosilane-functionalized silicon surfaces by microcontact printing; and (5) rapid preparation of a superhydrophobic hydrosilane-functionalized silicon nanowire (SiNW) surface. The combined results further establish the B-catalyzed siloxanation reaction as a prime method for covalently modifying these ubiquitously occurring silicon oxide surfaces.

## MATERIALS AND METHODS

**Chemicals.** n-Type phosphorus-doped silicon (111) wafers, with a resistivity of 0.01−0.018 Ω·cm, were used in these experiments. Heptadecafluoro-1,1,2,2-tetrahydrodecyl)dimethylchlorosilane (95% purum) was purchased from ABCR GmbH. Tris(pentafluorophenyl)-borane, chloro(dimethyl)octylsilane, chloro(decyl)dimethylsilane, chloro(dodecyl)dimethylsilane, chloro(dimethyl)octadecylsilane, acetone, diethyl ether, $CH_2Cl_2$, and $LiAlH_4$ (1 M in ether) were purchased from Sigma-Aldrich. Deionized (DI) water was obtained from a Milli-Q Integral water purification system (Merck-Millipore). Phosphate-buffered saline (PBS, 10 mM, pH 7.4) was prepared from a solution of NaCl (8.01 g/L), $Na_2HPO_4$ (1.41 g/L), $KH_2PO_4$ (0.27 g/L), and KCl (0.20 g/L) in DI water.

**General Procedure for the Synthesis of Hydrosilane Compounds.** The corresponding chloro(alkyl)dimethylsilane (40 mmol) was subjected to reduction by $LiAlH_4$ (36.8 mmol) in ether at 0 °C for 1 h. After reduction, the resultant mixture was quenched with $Na_2SO_4$·$10H_2O$ in an ice-cooled bath and filtered through a pad of Celite with $CH_2Cl_2$. The obtained clear solution was distilled under reduced pressure to give the corresponding alkyldimethylsilane $R(CH_3)_2Si$−H in high yield (95−98%).

**Characterization of Compounds and Surfaces.** Experimental details regarding characterization of the synthesized hydrosilanes **1**−**5**, including X-ray photoelectron spectroscopy (XPS), static water contact angle (SCA) measurements, atomic force microscopy (AFM), ellipsometry, and $^1H$ and $^{13}C$ NMR spectroscopies, can be found in the Supporting Information.

**Monolayer Preparation.** A piece of Si(111) wafer was first rinsed several times with acetone and then sonicated for 15 min in acetone. The Si wafer was then oxidized by air plasma cleaning (10 min), after which it was immersed in freshly prepared piranha solution ($H_2SO_4$/$H_2O_2$ 3:1) for 30 min at 60 °C. (*Note: Extreme caution is required in preparing, handling, and disposal of piranha solutions!*) After this piranha treatment, the substrates were immersed immediately in deionized water, rinsed thoroughly, and dried with a stream of nitrogen. Subsequently, the substrates were placed in a flask containing a $CH_2Cl_2$ solution of the hydrosilane and tris(pentafluorophenyl)borane (1 mol %) as the catalyst for 5 min at room temperature. After the reaction, the modified surfaces were rinsed and sonicated with $CH_2Cl_2$ for 15 min to remove any physisorbed compounds. The modified silicon substrates were directly used for surface characterization (XPS, IR, ellipsometry, and contact angle measurements).

**Hydrolytic Stability Experiments.** Hydrolytic stability tests were carried out by placing the modified surfaces in four different standardized aqueous environments in rubber-stoppered glass vials: deionized (DI) water, neutral PBS (pH 7.4), an acidic (HCl) solution at pH 3, and a basic (NaOH) solution at pH 11.[42] The vials under study were continuously agitated at 25 rpm at room temperature using an incubator shaker (benchtop Innova 4080) to mimic mechanical disturbances by flowing solvents; this approach also minimizes the deposition of adventitious carbon on the surface. The stability of the functionalized surfaces in acidic, basic, PBS, and neutral deionized water media was monitored by static water contact angle (SCA) measurements directly after preparation and after 1, 7, and 30 days of immersion in the described medium. In all cases, before the SCA measurements, the samples were taken from the medium, rinsed with fresh DI water, sonicated in water (5 min and subsequently in dichloromethane (also for 5 min), and finally rinsed with dichloromethane and dried in a flow of dry nitrogen. The samples were returned to new vials filled with freshly prepared solutions for prolonged periods of this stability study. The reported values are the averages of five surfaces.

**Computational Procedures.** All DFT calculations were carried out using Gaussian 09.[43] All geometries were fully optimized using the M11 functional[44] and the 6-311+G(d,p) basis set. Analytical



DOI: 10.1021/acs.langmuir.7b00110
Langmuir 2017, 33, 2185−2193

frequencies were calculated at this level, and the nature of the stationary points was determined. Initially, a Monte Carlo conformational search using the conformer distribution option available in Spartan'14 was used.[45] With this option, a search without constraints was performed for every structure. The torsion angles were varied randomly, and the obtained structures were fully optimized using the MMFF force field. Thus, 100 minima of energy within an energy gap of 10 kcal·mol$^{-1}$ were generated. These structures were analyzed and ordered considering the relative energy, with the repeated geometries eliminated. In all cases, all conformers within 4.0 kcal·mol$^{-1}$ of the lowest-energy conformer were studied quantum chemically. The results refer to that conformer that displayed the lowest energy in the quantum chemical calculations.

## RESULTS AND DISCUSSION

**Monolayer Preparation.** To study the grafting of hydrosilanes onto oxidized silicon surfaces catalyzed by the strongly Lewis acidic organoborane $B(C_6F_5)_3$ (Scheme 1), hydrosilanes bearing alkyl chains with different lengths [$CH_3$–$(CH_2)_n$–$CH_2$–$Si(CH_3)_2$–H, $n$ = 6–16] were synthesized in high yields [$C_8$ (**1**), $C_{10}$ (**2**), $C_{12}$ (**3**), and $C_{18}$ (**4**), Scheme 1] from the corresponding chloro(alkyl)dimethylsilanes by reduction with $LiAlH_4$, following a described procedure.[46] All of these hydrosilanes showed an intense IR band centered at 2111 cm$^{-1}$ assigned to the Si–H stretching mode, a multiplet in the $^1$H NMR spectra at 3.70–3.80 ppm corresponding to Si–H, and $^{13}$C NMR peaks between −4.4 and −5.0 ppm corresponding to Si–$CH_3$

Initially, Si(111) samples were cleaned and oxidized by acetone sonication, plasma cleaning (10 min), and oxidation in piranha solution ($H_2SO_4/H_2O_2$ 3:1). Next, the reaction between oxidized Si(111) and dimethyl(octyl)silane (**1**) in the presence of the boron catalyst was optimized using various conditions. All reactions were performed by immersing the freshly oxidized surface in a vial with 2 mL of dichloromethane solution containing 0.5 mmol of **1** (0.25 M). The control reaction performed in the absence of the aforementioned catalyst did not show an increase in the carbon content as measured by XPS (Table 1, entry 1), and the surface remained hydrophilic (SCA ≈ 10–12°). The addition of 5 mol % $B(C_6F_5)_3$ in the reaction mixture led to the formation of hydrogen (confirmed visually), which terminated within a few minutes. The samples reacted for 30 min (Table 1, entry 2) and 10 min (Table 1, entry 3) showed almost identical C/Si ratios (0.27 and 0.28, respectively), indicating that the reaction was completed within 5–10 min. Such grafting was also corroborated by an increase in the static water contact angle (SCA) from ∼10°, due to the hydrophilic hydroxyl groups across the OH-terminated surface, to 103° and the formation of an organic monolayer with a thickness of ∼0.8 nm as measured by ellipsometry and XPS (according to the C/Si ratio).[47] Lowering the catalyst loading to 1% continued to give similar C/Si ratios (Table 1, entry 4). Finally, it is worth mentioning that reaction also occurred in the absence of solvent (Table 1, entry 5). No changes in the XPS spectra were observed upon rinsing and sonication with $CH_2Cl_2$, suggesting the formation of covalently bound monolayers. The use of another Lewis acid, such as $BF_3$, was also studied (5 mol %, $CH_2Cl_2$); however, no surface modification was observed when this catalyst was used. Table 1 reports the XPS data, which revealed that the C/Si content increased notably relative to that of the unmodified substrate (Table 1, entry 1), indicating the effective grafting of the hydrosilane derivatives. Notably, both ellipsometry and XPS indicated the formation of a clean monolayer, without multilayer formation, as seen, for example, in the ellipsometry thickness values of about 0.86–0.91 nm and the XPS-inferred thickness (1.01 ± 0.20 nm for entry 5), in accordance with the expected thickness based on a fully stretched alkyl chain of this length (0.90 nm).

**Table 1. Optimization of the Reaction Conditions for the $B(C_6F_5)_3$-Catalyzed Attachment of Compound 1 onto Oxidized Si(111) Surfaces**

| entry | catalyst loading (mol %) | solvent | time (min) | C 1s (%) | C/Si ratio | thickness (nm)[a] |
|---|---|---|---|---|---|---|
| 1 | 0 | $CH_2Cl_2$ | 30 | 0.05 | <0.01 | <0.1 |
| 2 | 5 | $CH_2Cl_2$ | 30 | 15.2 | 0.27 | 0.88 ± 0.07 |
| 3 | 5 | $CH_2Cl_2$ | 10 | 15.4 | 0.28 | 0.91 ± 0.10 |
| 4 | 1 | $CH_2Cl_2$ | 10 | 14.7 | 0.28 | 0.86 ± 0.12 |
| 5 | 1 | none | 10 | 15.5 | 0.29 | 0.88 ± 0.07 |

[a]Thickness measured by ellipsometry.

A detailed study of the reaction time showed that the reaction was complete after 5–10 min, as confirmed by the XPS analysis of the C 1s region of **1**-derivatized surfaces for different reaction times (Figure 1B). Reaction times were similar to those reported for the $B(C_6F_5)_3$-catalyzed hydrosilane modification of amorphous mesoporous silica microparticles and hydroxyl-terminated porous silicon surfaces.[39,40] Small bubbles of hydrogen gas were observed evolving from the solution during the grafting procedure, in line with the reaction being dehydrogenative. As shown, the reaction time for the $B(C_6F_5)_3$-catalyzed attachment of hydrosilane compounds to oxidized silicon (5–10 min) is far superior to those of typical silanization reactions (2–18 h).[48−50]

**Monolayer Characterization.** Next, to study the influence of the alkyl chain length on the formation of the monolayer, the attachment of hydrosilanes bearing chains of different lengths [$CH_3$–$(CH_2)_n$–$CH_2$–$Si(CH_3)_2$–H, $n$ = 6–16] was studied under the optimized conditions [5 mol % $B(C_6F_5)_3$, 10 min]. Hydrosilane-modified silicon surfaces had SCAs between 103° and 111°, increasing with the hydrosilane chain length (Table 2). In particular, the SCA value for $C_{18}$-hydrosilane **4** of 111° corresponds to literature values reported for self-assembled monolayers of alkylsilanes on silicon oxide, indicating that the long-chain hydrosilane formed densely packed layers on the substrate surface.[51]

As reported in Table 2, the ellipsometric thicknesses $d_{Ellips}$ of the alkyl-terminated monolayers investigated in this study were found to be in accordance with those obtained by XPS ($d_{XPS}$, using the C/Si ratio) and similar to the expected thicknesses calculated for densely packed monolayers with fully extended molecules and a near-perpendicular orientation to the surface. No evidence of the formation of multilayers was found by ellipsometry or XPS, indicating a clean surface modification reaction, especially when compared to other solution-based chemistry modifications on oxidized silicon substrates, which usually require longer reaction times.[52]

Figure 2 shows the grazing-angle attenuated-total-reflectance infrared (GATR-IR) spectra of an ozone-oxidized Si surface and **1**–**4** hydrosilane-functionalized surfaces. Analysis of the $CH_2$ stretching vibrations of the prepared monolayers by GATR-IR spectroscopy revealed the absence of short-range ordering of the monolayers,[53] as shown by the antisymmetric and symmetric C–H stretching vibrations at 2927 and 2856 cm$^{-1}$, respectively (see Supporting Information, Table S1).



DOI: 10.1021/acs.langmuir.7b00110
Langmuir 2017, 33, 2185–2193

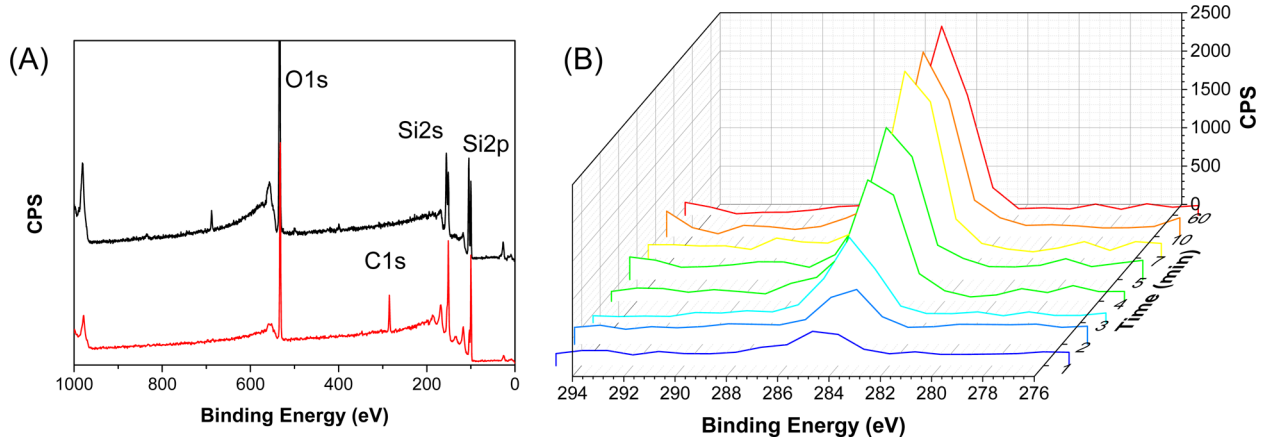


**Figure 1.** (A) XPS survey scans of an unmodified oxidized silicon surface after plasma and piranha treatment (black) and after modification with **1** (red). (B) Comparison of the XPS C 1s region of **1**-derivatized surfaces for different reaction times [1 mol % $B(C_6F_5)_3$].

**Table 2. Characteristics of Monolayers Derived from $B(C_6F_5)_3$-Catalyzed Attachment of Compounds 1–4 onto Oxidized Si(111): Static Water Contact Angles, XPS Data, and Monolayer Thicknesses (monolayer thicknesses are given in nm)[a]**

| hydrosilane | SCA (deg) | C 1s (%) | C/Si ratio | $d_{Ellips}$ [b] | $d_{XPS}$ [c] | $d_{theor}$ [d] |
|---|---|---|---|---|---|---|
| **1** | 103 | 15.5 | 0.29 | 0.91 ± 0.10 | 1.01 ± 0.20 | 0.90 |
| **2** | 106 | 15.9 | 0.30 | 1.12 ± 0.15 | 1.18 ± 0.20 | 1.11 |
| **3** | 108 | 16.2 | 0.32 | 1.38 ± 0.14 | 1.27 ± 0.15 | 1.33 |
| **4** | 111 | 25.4 | 0.54 | 1.97 ± 0.12 | 1.80 ± 0.21 | 1.98 |

[a]Using 5 mol % $B(C_6F_5)_3$ (10 min, room temperature). Each data point represents the average of five separately prepared monolayers. [b]Monolayer thickness as obtained by ellipsometry. [c]Monolayer thickness as obtained by XPS using the C/Si ratio. [d]Monolayer thickness as derived from Chem3D-estimated length of fully stretched chain.

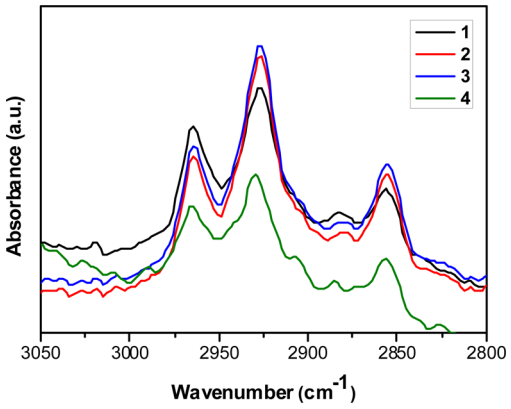


**Figure 2.** GATR-IR spectra of the $CH_2$ region of hydrosilane-functionalized Si surfaces.

This is attributed to the presence of Si-bound methyl groups.[54] The hydrosilane-modified silicon surfaces also showed a clear $CH_3$ stretching vibration at 2965 $cm^{-1}$.

The topography of Si surfaces after the $B(C_6F_5)_3$-catalyzed modification was studied by atomic force microscopy (AFM). The root-mean-square (rms) roughness of the bare Si(111) substrate was found to be 0.42 nm, which decreased to 0.10 nm after piranha cleaning. After hydrosilane grafting, a uniformly coated surface was observed with a roughness of <0.3 nm for all surfaces (see Supporting Information, Table S2). No evidence of islands or granules was observed in the AFM images, in accordance with the presence of a fully formed monolayer on the surface.

**Quantum Chemical Studies of Possible Mechanism.** Whereas the $B(C_6F_5)_3$-catalyzed hydrosilylation of carbonyl compounds has been examined in detail both experimentally[55,56] and theoretically,[57] no computational studies on the catalytic activation of hydrosilanes and their novel reactions with oxidized silicon substrates have been performed. A mechanism for this grafting procedure based on previous reports on Si–H activation by borane compounds along the lines proposed by Nakanishi and Shimada[39] involves the formation of a highly active intermediate by reaction of the $B(C_6F_5)_3$ catalyst with the hydrosilane (Figure 3A; intermediate **I**). The silicon atom in this intermediate is electron-deficient and therefore attacks the electron-rich silanol oxygen atom at the silica surface, which has acidic character ($pK_a$ = 4.9–8.5), to form an anionic species and a cationic intermediate (intermediate **IV**). Finally, the basic hydride intermediate abstracts a proton from silanol groups or the cationic intermediate, thereby regenerating the catalyst and yielding the immobilized product and hydrogen gas (as observed experimentally).

On the basis of this mechanism, we examined a model reaction system consisting of dimethyl(propyl)silane (**6**) and a glass model surface [$Si(OH)_4$] to reveal how the silane is activated by $B(C_6F_5)_3$. First, the noncatalyzed reaction was studied quantum mechanically by M11/6-311+G(d,p) calculations. (Cartesian coordinates of all stationary points as obtained at this level of theory are given in Supporting Information section 6.) This reaction involved a high activation barrier of 44.8 kcal/mol, in agreement with the observation that no reaction was observed at room temperature in the absence of $B(C_6F_5)_3$. Next, we examined the $B(C_6F_5)_3$-catalyzed reaction, assuming that this Lewis acid activates the hydrosilane[56] and effects the formation of a complex between $B(C_6F_5)_3$ and hydrosilane molecule with a linear Si–H–B bond arrangement. In our case, the calculations showed the


DOI: 10.1021/acs.langmuir.7b00110
Langmuir 2017, 33, 2185–2193

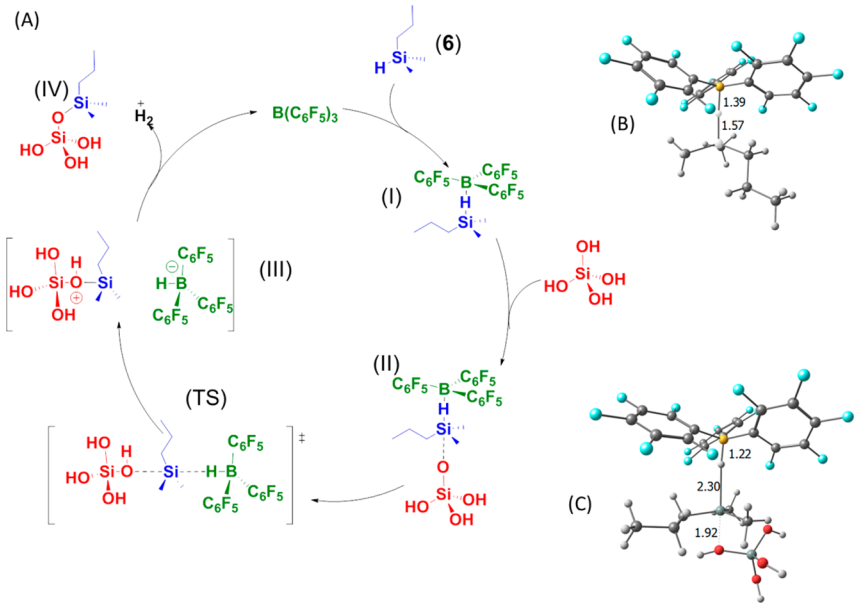


**Figure 3.** (A) Proposed catalytic cycle and (B,C) optimized structures of (B) intermediate **I** and (C) transition state **TS** for the $B(C_6F_5)_3$-catalyzed dedihydrosiloxanation on oxidized silicon surfaces at the M11/6-311G+(d,p) level of theory. Bond lengths are given in angstroms.

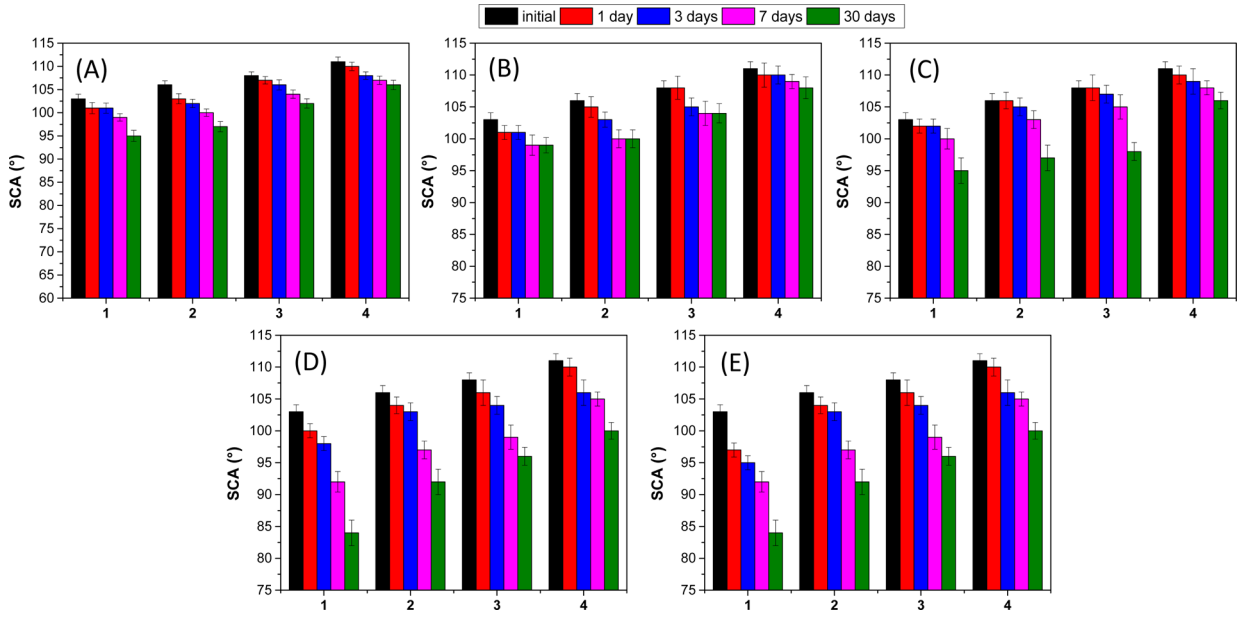


**Figure 4.** Hydrolytic stability as followed by SCA monolayers derived from **1**–**4** on oxidized Si(111) in (A) deionized water, (B) neutral PBS (pH 7.4), (C) an acidic solution (pH 3), (D) a basic solution (pH 11), and (E) thermal stability under dry heating in air (130 °C). The reported values are the averages of five surfaces.

formation of borane–hydrosilane adduct **I** with a calculated complexation free energy of 18.1 kcal/mol with respect to the reactants. As illustrated in Figure 3B, a relatively strong and near-linear Si···H···B interaction between $B(C_6F_5)_3$ and dimethyl(propyl)silane can be observed, with Si–H and B–H bond distances of 1.57 and 1.39 Å, respectively.

The next step in the process involves the approach of the electron-rich oxygen of a silanol from the oxidized silicon surface to the back side of the Si–H bond in the now electron-deficient Si atom of the borane–hydrosilane intermediate **I** to form reactant complex **II**. In this intermediate, the distance between the silicon from the hydrosilane and the silanol oxygen is still 2.58 Å, and the B–H distance has been shortened to 1.34 Å, whereas the Si–H distance has been lengthened to 1.62 Å. Further approach of the oxygen to the silicon atom gives rise to transition state **TS** involving a small barrier of 7.9 kcal/mol, with Si–H and B–H distances of 2.30 and 1.22 Å, respectively. In this TS structure, the Si–O distance was found to be 1.92 Å (Figure 3C). Finally, the **TS** can give the acidic and cationic intermediate **III**, which, after proton transfer and $H_2$ formation, forms the product and regenerates the $B(C_6F_5)_3$ catalyst.

**Thermal and Hydrolytic Stability.** The hydrolytic stability of the hydrosilane-derived monolayers was studied under standardized "continuous-flow" conditions in four different aqueous media [deionized water, PBS (pH 7.4), HCl solution of pH 3, and NaOH solution at pH 11].[42] After 1,



DOI: 10.1021/acs.langmuir.7b00110
Langmuir 2017, 33, 2185–2193

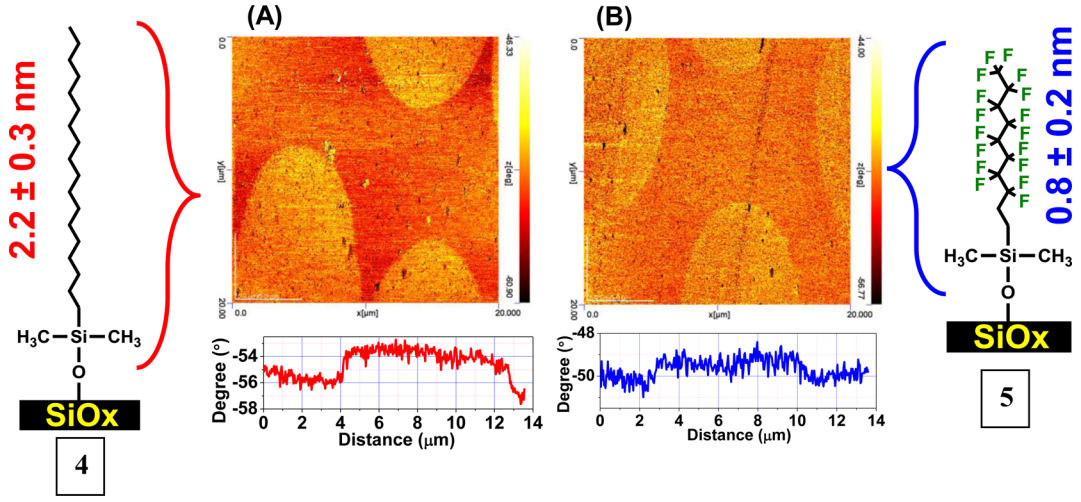


**Figure 5.** AFM phase images of the patterned monolayers with hydrosilane (A) **4** and (B) **5**, together with AFM topography-determined thicknesses.

3, 7, and 30 days, samples were cleaned and sonicated in water, following a standardized procedure. The hydrolytic stability was followed by SCA measurements (Figure 4) and by carbon desorption rates, using the C/Si ratio from XPS survey scans; in each case, data were normalized to the value of the surface as obtained directly after modification. After immersion for 1 or 3 days in all four solutions, no major changes were observed in the SCA or in the carbon percentage as determined by XPS with respect to the starting situation. After immersion for 3 days in $H_2O$, PBS, and pH 3 solutions, the contact angle dropped slightly (2−3°), and the XPS C/Si ratio decreased by ~4%. Even after 7 days of immersion in neutral or acidic media, only minor changes were detected, whereas only in basic solution was an SCA reduction of 7° observed, in line with the 6% reduction of the percentage C content as determined by XPS. In water (Figure 4A) and physiological PBS solution (Figure 4B), no significant decrease in SCA was observed after a week (about 4° decrease), and only after 30 days was a decrease of 6° measured for monolayers containing compounds **1**, **2**, and **3**; this effect was even smaller for the longer-chain monolayer, with only a 4° decrease. These results show the high stability of the monolayers, which hardly suffered from any hydrolysis under the studied conditions.

Under acidic conditions (Figure 4C), the water SCA showed very little change after 7 days and remained high, on average, even after 30 days. Here, the effect of chain length was more pronounced, as a decrease of 8−10° was measured for monolayers containing hydrosilanes **1**, **2**, and **3** after 30 days. The XPS data also showed a significant reduction of the C signal in these functionalized surfaces after 30 days at pH 3. In contrast, **4**-functionalized monolayers showed only a 5° decrease. These results are similar to those found for an octadecylsilane monolayer on glass[42] and alkylphosphonic acid monolayers attached to stainless steel.[58]

Finally, in contrast to the high stability shown in physiological solution (PBS buffer) and acidic media, the stability under basic conditions (pH 11) was found to be lower, especially for the shorter **1**-functionalized monolayer (Figure 4D), with a decrease in contact angle of 6% (from 103° to 100°) after 1 day, in contrast to the decrease of 1−2% for the other monolayers under study. This lower stability was also observed as the study was prolonged along 3, 7, and 30 days, indicating the hydrolysis of the shortest monolayer under study, with a total decrease of about 18% (from 103° to 84°) after 30 days. For the rest of the monolayers, the SCA remained above 92° after 30 days at pH 11. In particular, for the **4**-functionalized monolayers, a higher stability was found (SCA > 100°) when compared to that of the $C_{18}$ monolayers prepared with chlorosilanes, and the stability was at least as good as that obtained for extensively cured (up to 120 h at 80 °C) phosphonate-bound $C_{18}$ monolayers.[42,59] These results clearly show the potential of this surface modification as reaction times are significantly shorter than those of other well-established surface modification strategies.

Finally, the thermal stability of the different monolayers was studied at 130 °C in air. As observed in Figure 4E, exposure to heat for 1 or 3 days caused a decrease of only a few degrees in the SCA. Only upon extended heating (30 days at 130 °C) was the SCA decreased by 18°, 13°, 13°, and 11° for surfaces modified with **1**, **2**, **3**, and **4**, respectively, with the value for the octyldecyl layer still >100°. Such length dependence was not as clearly observed for $O_3Si$−C-bound trichlorosilane-derived monolayers, in which the heating also could effect additional curing, which was, of course, absent here.

**Microcontact Printing.** Given the high reaction rates, hydrosilane attachment might be of significant interest for reactive microcontact printing. Therefore, we investigated the microcontact printing of hydrosilanes onto freshly oxidized silicon surfaces. A polydimethylsiloxane (PDMS) stamp with 10-mm pillar-like features was prepared by curing a commercially available PDMS prepolymer on a patterned master. The PDMS was next covered with a mixture of hydrosilane **4** and 1 mol % $B(C_6F_5)_3$ in dichloromethane and subsequently brought into contact with the oxidized silicon substrate for 30 s. After thorough cleaning of the substrate, the surface displayed a 10-$\mu$m sphere pattern in the AFM phase image, confirming successful transfer of the pattern, as shown in Figure 5A. The average thickness calculated by AFM corresponded a monolayer of 2.2 ± 0.3 nm. When the shorter hydrosilane **5** was used, a thickness of 0.8 ± 0.2 nm was measured for this monolayer (Figure 5B). The short (30-s) reaction time required for the microcontact printing approach shows the potential of the hydrosilane attachment reaction to functionalize and pattern oxidized silicon surfaces.

**Silicon Nanowire Modification.** Given the importance of silicon nanowires in the design of sensors, solar cells, and



DOI: 10.1021/acs.langmuir.7b00110
*Langmuir* 2017, 33, 2185−2193

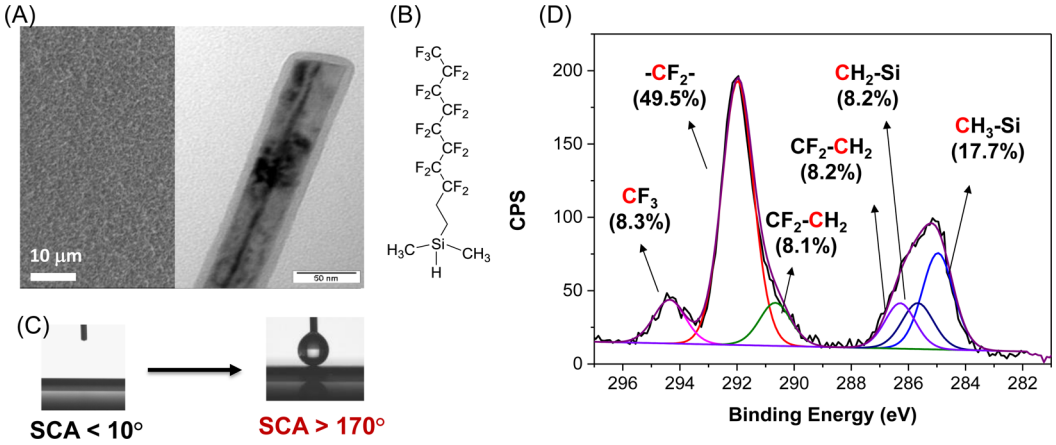


**Figure 6.** (A) SEM image of a SiNW forest by "bottom-up" fabrication with lengths of 45−50 $\mu$m and TEM image of a single nanowire. (B) Chemical structure of hydrosilane **5**. (C) SCA images before (left) and after (right) $B(C_6F_5)_3$-catalyzed modification (5 min, room temperature) of SiNWs with hydrosilane **5**. (D) C 1s XPS spectra of SiNWs coated with a monolayer of hydrosilane **5**.

superhydrophobic surfaces and the high reaction rates of hydrosilanes, which sharply reduce handling times, we extended this protocol to modify SiNWs. Toward this end, SiNWs were prepared on Si(111) surfaces by chemical vapor deposition of $B_2H_6$ and $SiH_4$ (B/Si atom ratio of 1:20000) as precursor gases and gold as a catalyst.[60] For the surface modification, the SiNWs were initially cleaned with plasma and piranha solution to activate the surface Si−OH groups. After the reaction (5 min, room temperature) with a mixture of **4** and 1 mol % $B(C_6F_5)_3$, the SiNWs became highly hydrophobic: The SCA increased from an initial value of less than 10° to a final value of 145°. More interestingly, a superhydrophobic surface was obtained when a (perfluorooctyl)hydrosilane **5** (thus bearing a $C_8F_{17}$ chain) was used, with a final SCA of 170° (Figure 6C). The successful modification of SiNWs was further corroborated by XPS. After reaction with **5** (Figure 6B), clear increases in the percentages of C and F were observed, confirming the effective grafting of the fluorinated compound. The XPS F/C atomic ratio calculated as an average of three different fluorinated-modified surfaces was 1.40 ± 0.12, in excellent agreement with the theoretical value of 1.42. A detailed investigation of the XPS C 1s spectra confirmed the successful monolayer formation, as shown by peak deconvolution into different components corresponding to the carbon atoms having different environments. As shown in Figure 5D, the C 1s spectrum was deconvoluted into six peaks in line with the monolayer structure: the $Si-CH_3$ peak at 285.0 eV and peaks for $-\underline{C}H_2-Si$, $-CH_2-\underline{C}H_2-CF_2$, $-\underline{C}F_2-CH_2-$, $-\underline{C}F_2-$, and the terminal $-\underline{C}F_3$ at 285.8, 286.7, 291.3, 292.0, and 294.4 eV, respectively.

This approach represents one of the fastest methods for functionalizing oxide-coated SiNWs, as most of the approaches based on silanization reactions typically require long reaction times (from 3 to 24 h). Consequently, this rapid functionalization might have a wide range of potential applications because of its speed and the use of a nonmetallic catalyst.

## CONCLUSIONS

The formation of robust and covalently bound organic monolayers on oxidized silicon surfaces can be rapidly (5−10 min) achieved at room temperature through hydrosilane attachment as catalyzed by $B(C_6F_5)_3$. Hydrosilanes $H-Si(CH_3)_2R$ with alkyl chains R containing from 8 to 18 carbon atoms form highly stable self-assembled monolayers, as evidenced by 30-day-long testing in various media. As a proof of concept, we applied this methodology to functionalize SiNWs, and superhydrophobic surfaces were rapidly obtained using fluorinated hydrosilanes. A quantum chemical study of the catalyzed reaction pathway showed that the $B(C_6F_5)_3$ catalyst coordinates to the hydrosilane to form a stable B···H−Si complex. This activated silane complex undergoes a back-side attack from the surface-bound Si−OH group to form a Si−O−Si bond, which finally yields the immobilized product and hydrogen. The catalyst reduces the activation barrier from 45 to 18 kcal/mol, yielding hydrosilanes as mild yet highly reactive monolayer-forming agents.

## ASSOCIATED CONTENT

### Supporting Information

The Supporting Information is available free of charge on the ACS Publications website at DOI: 10.1021/acs.langmuir.7b00110.

Experimental details regarding characterization of the synthesized hydrosilanes **1**−**5** by X-ray photoelectron spectroscopy (XPS), static water contact angle (SCA) measurements, atomic force microscopy (AFM), ellipsometry, and $^1H$ and $^{13}C$ NMR spectroscopies. Cartesian coordinates of stationary points at the M11/6-311+G-(d,p) level of theory (PDF)

## AUTHOR INFORMATION

### Corresponding Author

*E-mail: han.zuilhof@wur.nl.

### ORCID

Sidharam P. Pujari: 0000-0003-0479-8884

Han Zuilhof: 0000-0001-5773-8506

### Author Contributions

The manuscript was written through contributions of all authors. All authors have given approval to the final version of the manuscript.

### Notes

The authors declare no competing financial interest.



DOI: 10.1021/acs.langmuir.7b00110
Langmuir 2017, 33, 2185−2193

## ■ ACKNOWLEDGMENTS

The authors thank NanoNext Program 3E and 6C for partial funding of this project.

## ■ REFERENCES

(1) Regli, S.; Kelly, J. A.; Barnes, M. A.; Andrei, C. M.; Veinot, J. G. C. Mesoporous silica encapsulation of silicon nanocrystals: synthesis, aqueous dispersibility and drug release. *Mater. Lett.* **2014**, *115*, 21−24.
(2) Peng, F.; Cao, Z.; Ji, X.; Chu, B.; Su, Y.; He, Y. Silicon nanostructures for cancer diagnosis and Therapy. *Nanomedicine* **2015**, *10*, 2109−2123.
(3) Wang, J.; Zhou, Y.; Watkinson, M.; Gautrot, J.; Krause, S. High sensitivity light-addressable potentiometric sensors using silicon on sapphire functionalized with self-assembled organic monolayers. *Sens. Actuators, B* **2015**, *209*, 230−236.
(4) Urmann, K.; Walter, J.-G.; Scheper, T.; Segal, E. Label-free optical biosensors based on aptamer-functionalized porous silicon scaffolds. *Anal. Chem.* **2015**, *87*, 1999−2006.
(5) Pujari, S. P.; Scheres, L.; Marcelis, A. T. M.; Zuilhof, H. Covalent surface modification of oxide surfaces. *Angew. Chem., Int. Ed.* **2014**, *53*, 6322−6356.
(6) Walters, R. J.; Bourianoff, G. I.; Atwater, H. A. Field-effect electroluminescence in silicon nanocrystals. *Nat. Mater.* **2005**, *4*, 143−146.
(7) Peng, W.; Rupich, S. M.; Shafiq, N.; Gartstein, Y. N.; Malko, A. V.; Chabal, Y. J. Silicon surface modification and characterization for emergent photovoltaic applications based on energy transfer. *Chem. Rev.* **2015**, *115*, 12764−12796.
(8) Ding, Y.; Dong, Y.; Bapat, A.; Nowak, J. D.; Carter, C. B.; Kortshagen, U. R.; Campbell, S. A. Single nanoparticle semiconductor devices. *IEEE Trans. Electron Devices* **2006**, *53*, 2525−2531.
(9) Gooding, J. J.; Ciampi, S. The molecular level modification of surfaces: from self-assembled monolayers to complex molecular assemblies. *Chem. Soc. Rev.* **2011**, *40*, 2704−2718.
(10) Aswal, D. K.; Lenfant, S.; Guerin, D.; Yakhmi, J. V.; Vuillaume, D. Self-assembled monolayers on silicon for molecular electronics. *Anal. Chim. Acta* **2006**, *568*, 84−108.
(11) Chen, W.; McCarthy, T. J. Layer-by-layer deposition: a tool for polymer surface modification. *Macromolecules* **1997**, *30*, 78−86.
(12) Wang, Y.; Angelatos, A. S.; Caruso, F. Template synthesis of nanostructured materials via layer-by-layer assembly. *Chem. Mater.* **2008**, *20*, 848−858.
(13) Yao, S. A.; Ruther, R. E.; Zhang, L. H.; Franking, R. A.; Hamers, R. J.; Berry, J. F. Covalent attachment of catalyst molecules to conductive diamond: $CO_2$ reduction using "smart" electrodes. *J. Am. Chem. Soc.* **2012**, *134*, 15632−15635.
(14) Haensch, C.; Hoeppener, S.; Schubert, U. S. Chemical modification of self-assembled silane based monolayers by surface reactions. *Chem. Soc. Rev.* **2010**, *39*, 2323−2334.
(15) Klein, R. J.; Fischer, D. A.; Lenhart, J. L. Thermal and mechanical aging of self-assembled monolayers as studied by near edge X-ray absorption fine structure. *Langmuir* **2011**, *27*, 12423−12433.
(16) Dugas, V.; Chevalier, Y. Chemical Reactions in Dense Monolayers: In situ thermal cleavage of grafted esters for preparation of solid surfaces functionalized with carboxylic acids. *Langmuir* **2011**, *27*, 14188−14200.
(17) Pasternack, R. M.; Rivillon Amy, S.; Chabal, Y. J. Attachment of 3-(aminopropyl)triethoxysilane on silicon oxide surfaces: dependence on solution temperature. *Langmuir* **2008**, *24*, 12963−12971.
(18) Kuroda, K.; Shimojima, A.; Kawahara, K.; Wakabayashi, R.; Tamura, Y.; Asakura, Y.; Kitahara, M. Utilization of alkoxysilyl groups for the creation of structurally controlled siloxane-based nanomaterials. *Chem. Mater.* **2014**, *26*, 211−220.
(19) Shimada, T.; Aoki, K.; Shinoda, Y.; Nakamura, T.; Tokunaga, N.; Inagaki, S.; Hayashi, T. Functionalization on silica gel with allylsilanes. A new method of covalent attachment of organic functional groups on silica gel. *J. Am. Chem. Soc.* **2003**, *125*, 4688−4689.
(20) Park, J.-W.; Jun, C.-H. Transition-metal-catalyzed immobilization of organic functional groups onto solid supports through vinylsilane coupling reactions. *J. Am. Chem. Soc.* **2010**, *132*, 7268−7269.
(21) Lee, A. W. H.; Gates, B. D. Rapid Covalent Modification of Silicon Oxide Surfaces through Microwave-Assisted Reactions with Alcohols. *Langmuir* **2016**, *32*, 7284−7293.
(22) Carvalho, R. R.; Pujari, S. P.; Lange, S. C.; Sen, R.; Vrouwe, E. X.; Zuilhof, H. Local Light-Induced Modification of the Inside of Microfluidic Glass Chips. *Langmuir* **2016**, *32*, 2389−2398.
(23) Carvalho, R. R.; Pujari, S. P.; Gahtory, D.; Vrouwe, E. X.; Albada, B.; Zuilhof, H. Mild Photochemical Biofunctionalization of Glass Microchannels. *Langmuir* **2017**, DOI: 10.1021/acs.langmuir.6b03931.
(24) Jung, G.-Y.; Li, Z.; Wu, W.; Chen, Y.; Olynick, D. L.; Wang, S.-Y.; Tong, W. M.; Williams, R. S. Vapor-phase self-assembled monolayer for improved mold release in nanoimprint lithography. *Langmuir* **2005**, *21*, 1158−1161.
(25) Alekseev, S. A.; Lysenko, V.; Zaitsev, V. N.; Barbier, D. Application of infrared interferometry for quantitative analysis of chemical groups grafted onto the internal surface of porous silicon nanostructures. *J. Phys. Chem. C* **2007**, *111*, 15217−15222.
(26) Escorihuela, J.; Marcelis, A. T. M.; Zuilhof, H. Metal-Free Click Chemistry Reactions on Surfaces. *Adv. Mater. Interfaces* **2015**, *2*, 1500135.
(27) Mikolajick, T.; Heinzig, A.; Trommer, J.; Pregl, S.; Grube, M.; Cuniberti, G.; Weber, W. M. Silicon nanowires−a versatile technology platform. *Phys. Status Solidi RRL* **2013**, *7*, 793−799.
(28) Zhang, B.-C.; Wang, H.; Zhao, Y.; Li, F.; Ou, X.-M.; Sun, B.-Q.; Zhang, X.-H. Large-scale assembly of highly sensitive Si-based flexible strain sensors for human motion monitoring. *Nanoscale* **2016**, *8*, 2123−2128.
(29) Kempa, T. J.; Day, R. W.; Kim, S.-K.; Park, H.-G.; Lieber, C. M. Semiconductor nanowires: a platform for exploring limits and concepts for nano-enabled solar cells. *Energy Environ. Sci.* **2013**, *6*, 719−733.
(30) Tian, B. Z.; Kempa, T. J.; Lieber, C. M. Single nanowire photovoltaics. *Chem. Soc. Rev.* **2009**, *38*, 16−24.
(31) Wu, H.; Cui, Y. Designing nanostructured Si anodes for high energy lithium ion batteries. *Nano Today* **2012**, *7*, 414−429.
(32) Coffinier, Y.; Janel, S.; Addad, A.; Blossey, R.; Gengembre, L.; Payen, E.; Boukherroub, R. Preparation of superhydrophobic silicon oxide nanowire surfaces. *Langmuir* **2007**, *23*, 1608−1611.
(33) Xu, W. L.; Vegunta, S. S. S.; Flake, J. C. Surface-modified silicon nanowire anodes for lithium ion batteries. *J. Power Sources* **2011**, *196*, 8583−8589.
(34) Hahm, J.; Lieber, C. M. Direct Ultrasensitive electrical detection of DNA and DNA sequence variations using nanowire nanosensors. *Nano Lett.* **2004**, *4*, 51−54.
(35) Cattani-Scholz, A.; Pedone, D.; Dubey, M.; Neppl, S.; Nickel, B.; Feulner, P.; Schwartz, J.; Abstreiter, G.; Tornow, M. Organophosphonate-based PNA-functionalization of silicon nanowires for label-free DNA detection. *ACS Nano* **2008**, *2*, 1653−1660.
(36) Bunimovich, Y. L.; Shin, Y. S.; Yeo, W. S.; Amori, M.; Kwong, G.; Heath, J. R. Quantitative real-time measurements of DNA hybridization with alkylated nonoxidized silicon nanowires in electrolyte solution. *J. Am. Chem. Soc.* **2006**, *128*, 16323−16331.
(37) Zhang, G. J.; Zhang, G.; Chua, J. H.; Chee, R. E.; Wong, E. H.; Agarwal, A.; Buddharaju, K. D.; Singh, N.; Gao, Z. Q.; Balasubramanian, N. DNA sensing by silicon nanowire: charge layer distance dependence. *Nano Lett.* **2008**, *8*, 1066−1070.
(38) Nguyen Minh, Q.; Wang, B.; Pujari, S. P.; Wang, Z.; Haick, H.; Zuilhof, H.; van Rijn, C. J. M. Fluorinated alkyne-derived monolayers on oxide−free silicon nanowires: formation and performance in field effect transistor. *Appl. Surf. Sci.* **2016**, *387*, 1202−1210.
(39) Moitra, N.; Ichii, S.; Kamei, T.; Kanamori, K.; Zhu, Y.; Takeda, K.; Nakanishi, K.; Shimada, T. Surface Functionalization of silica by Si−H activation of hydrosilanes. *J. Am. Chem. Soc.* **2014**, *136*, 11570−11573.



DOI: 10.1021/acs.langmuir.7b00110
*Langmuir* 2017, 33, 2185−2193

(40) Sweetman, M. J.; McInnes, S. J. P.; Vasani, R. B.; Guinan, T.; Blencowe, A.; Voelcker, N. H. Rapid, metal-free hydrosilanisation chemistry for porous silicon surface modification. *Chem. Commun.* **2015**, *51*, 10640−10643.
(41) Förch, R.; Schönherr, H.; Jenkins, A. T. A. *Surface Design: Applications in Bioscience and Nanotechnology*; Wiley-VCH Verlag GmbH & Co. KGaA: Weinheim, Germany, 2009.
(42) Bhairamadgi, N. S.; Pujari, S. P.; Trovela, F. G.; Debrassi, A.; Khamis, A. A.; Alonso, J. M.; Al Zahrani, A. A.; Wennekes, T.; Al-Turaif, H. A.; van Rijn, C.; Alhamed, Y. A.; Zuilhof, H. Hydrolytic and thermal stability of organic monolayers on various inorganic substrates. *Langmuir* **2014**, *30*, 5829−5839.
(43) Frisch, M. J.; Trucks, G. W.; Schlegel, H. B.; Scuseria, G. E.; Robb, M. A.; Cheeseman, J. R.; Scalmani, G.; Barone, V.; Mennucci, B.; Petersson, G. A.; Nakatsuji, H.; Caricato, M.; Li, X.; Hratchian, H. P.; Izmaylov, A. F.; Bloino, J.; Zheng, G.; Sonnenberg, J. L.; Hada, M.; Ehara, M.; Toyota, K.; Fukuda, R.; Hasegawa, J.; Ishida, M.; Nakajima, T.; Honda, Y.; Kitao, O.; Nakai, H.; Vreven, T.; Montgomery, J. A., Jr.; Peralta, J. E.; Ogliaro, F.; Bearpark, M.; Heyd, J. J.; Brothers, E.; Kudin, K. N.; Staroverov, V. N.; Keith, T.; Kobayashi, R.; Normand, J.; Raghavachari, K.; Rendell, A.; Burant, J. C.; Iyengar, S. S.; Tomasi, J.; Cossi, M.; Rega, N.; Millam, J. M.; Klene, M.; Knox, J. E.; Cross, J. B.; Bakken, V.; Adamo, C.; Jaramillo, J.; Gomperts, R.; Stratmann, R. E.; Yazyev, O.; Austin, A. J.; Cammi, R.; Pomelli, C.; Ochterski, J. W.; Martin, R. L.; Morokuma, K.; Zakrzewski, V. G.; Voth, G. A.; Salvador, P.; Dannenberg, J. J.; Dapprich, S.; Daniels, A. D.; Farkas, Ö.; Foresman, J. B.; Ortiz, J. V.; Cioslowski, J.; Fox, D. J. *Gaussian 09*, revision D.01; Gaussian, Inc.: Wallingford, CT, 2009.
(44) Peverati, R.; Truhlar, D. G. Improving the Accuracy of Hybrid Meta-GGA Density Functionals by Range Separation. *J. Phys. Chem. Lett.* **2011**, *2*, 2810−2817.
(45) *Spartan'14*; Wavefunction, Inc.: Irvine, CA, 2014. See also http://www.wavefun.com.
(46) Daiss, J. O.; Duda-Johner, S.; Burschka, C.; Holzgrabe, U.; Mohr, K.; Tacke, R. N+/Si replacement as a tool for probing the pharmacophore of allosteric modulators of muscarinic $M_2$ receptors: synthesis, allosteric potency, and positive cooperativity of silicon-based W84 Derivatives. *Organometallics* **2002**, *21*, 803−811.
(47) Rijksen, B.; Pujari, S. P.; Scheres, L.; van Rijn, C. J.; Baio, J. E.; Weidner, T.; Zuilhof, H. Hexadecadienyl monolayers on hydrogen-terminated Si(111): faster monolayer formation and improved surface coverage using the enyne moiety. *Langmuir* **2012**, *28*, 6577−6588.
(48) Escorihuela, J.; Bañuls, M. J.; Puchades, R.; Maquieira, A. DNA microarrays on silicon surfaces through thiol-ene chemistry. *Chem. Commun.* **2012**, *48*, 2116−2118.
(49) Escorihuela, J.; Bañuls, M.-J.; Puchades, R.; Maquieira, A. Development of oligonucleotide microarrays onto Si-based surfaces via thioether linkage mediated by UV irradiation. *Bioconjugate Chem.* **2012**, *23*, 2121−2128.
(50) Escorihuela, J.; Bañuls, M.-J.; Puchades, R.; Maquieira, A. Site-specific immobilization of DNA on silicon surfaces by using the thiol-yne reaction. *J. Mater. Chem. B* **2014**, *2*, 8510−8517.
(51) Ulman, A. *An Introduction to Ultrathin Organic Films: From Langmuir−Blodgett to Self-Assembly*; Academic Press: San Diego, CA, 1991.
(52) Wang, M.; Liechti, K. M.; Wang, Q.; White, J. M. Self-assembled silane monolayers: fabrication with nanoscale uniformity. *Langmuir* **2005**, *21*, 1848−1857.
(53) Nuzzo, R. G.; Dubois, L. H.; Allara, D. L. Fundamental studies of microscopic wetting on organic surfaces. 1. Formation and structural characterization of a self-consistent series of polyfunctional organic monolayers. *J. Am. Chem. Soc.* **1990**, *112*, 558−569.
(54) Scheres, L.; Giesbers, M.; Zuilhof, H. Organic monolayers onto oxide-free silicon with improved surface coverage: alkynes versus alkenes. *Langmuir* **2010**, *26*, 4790−4795.
(55) Parks, D. J.; Piers, W. E. Tris(pentafluorophenyl)boron-catalyzed hydrosilation of aromatic aldehydes, ketones, and esters. *J. Am. Chem. Soc.* **1996**, *118*, 9440−9441.
(56) Parks, D. J.; Blackwell, J. M.; Piers, W. E. Studies on the mechanism of $B(C_6F_5)_3$-catalyzed hydrosilation of carbonyl functions. *J. Org. Chem.* **2000**, *65*, 3090−3098.
(57) Sakata, K.; Fujimoto, H. Quantum chemical study of $B(C_6F_5)_3$-catalyzed hydrosilylation of carbonyl group. *J. Org. Chem.* **2013**, *78*, 12505−12512.
(58) Kosian, M.; Smulders, M. M. J.; Zuilhof, H. Structure and long-term stability of alkylphosphonic acid monolayers on SS316L stainless steel. *Langmuir* **2016**, *32*, 1047−1057.
(59) Marcinko, S.; Fadeev, A. Y. Hydrolytic stability of organic monolayers supported on $TiO_2$ and $ZrO_2$. *Langmuir* **2004**, *20*, 2270−2273.
(60) Stelzner, T.; Andrä, G.; Wendler, E.; Wesch, W.; Scholz, R.; Gösele, U.; Christiansen, S. Growth of silicon nanowires by chemical vapour deposition on gold implanted silicon substrates. *Nanotechnology* **2006**, *17*, 2895−2898.


DOI: 10.1021/acs.langmuir.7b00110
*Langmuir* 2017, 33, 2185−2193